Identification of a Cyanine-Dye Labelled Peptidic Ligand for Y_1R and Y_4R, Based upon the Neuropeptide Y C-terminal Analogue, BVD-15.

Mengjie Liu,[a] Rachel R. Richardson,[c] Simon J. Mountford,[a] Lei Zhang,[b] Matheus H. Tempone,[c] Herbert Herzog,[b] Nicholas D. Holliday,[c]* Philip E. Thompson.[a]*

a. Medicinal Chemistry, Monash Institute of Pharmaceutical Sciences, Monash University, 381 Royal Parade, Parkville, VIC 3052, Australia.

b. Neuroscience Research Program, Garvan Institute of Medical Research, St. Vincent's Hospital, Darlinghurst, NSW 2010, Australia.

c. Cell Signalling Research Group, School of Life Sciences, University of Nottingham, Queen's Medical Centre, Nottingham, NG7 2UH, UK.

* Corresponding Authors:

philip.thompson@monash.edu, Tel: +61 3 99039672, Fax: +61 3 99039582
nicholas.holliday@nottingham.ac.uk, Tel: +44 115 82 30084, Fax: +44 115 82 30081

Abstract

Traceable truncated Neuropeptide Y (NPY) analogues with Y_1 receptor (Y_1R) affinity and selectivity are highly desirable tools in studying receptor location, regulation and biological functions. A range of fluorescently labelled analogues of a reported Y_1R/Y_4R preferring ligand BVD-15 have been prepared and evaluated using high content imaging techniques. One peptide, [Lys^2(sCy5), Arg^4]BVD-15, was characterised as an Y_1R antagonist with a pK_D of 7.2 measured by saturation analysis using fluorescent imaging. The peptide showed 8-fold lower affinity for Y_4R (pK_D = 6.2) and was a partial agonist at this receptor. The suitability of [Lys^2(sCy5), Arg^4]BVD-15 for Y_1R and Y_4R competition binding experiments was also demonstrated in intact cells. The nature of the label was shown to be critical with replacement of sCy5 by the more hydrophobic Cy5.5 resulting in a switch from Y_1R antagonist to Y_1R partial agonist.

Introduction

Neuropeptide Y (NPY) is a 36-amino acid, C-terminal amidated polypeptide first isolated from porcine brain by Tatemoto's group in 1982.[1] It is a member of the NPY peptide family along with pancreatic polypeptide (PP, isolated in 1983)[2] and peptide YY (PYY, isolated in 1980)[3], which both share a high degree of homology in amino acid sequence. The physiological functions of NPY are mediated by Y receptors, belonging to the rhodopsin-like G_i coupled G-protein coupled receptor (GPCR) family and four subtypes, Y_1R, Y_2R, Y_4R and Y_5R have been identified in humans.[4-6] Y_1R is expressed abundantly in both central and peripheral sympathetic nervous systems, and the NPY/Y_1R signalling cascade is implicated in various physiological responses, including regulation of feeding behaviour,[7, 8] stimulation of ethanol intake,[9, 10] vasoconstriction[11, 12] and initiation of anxiety and depression.[13, 14] In addition, breast carcinomas, including primary tumours and lymph node metastases, have also been found to over-express Y_1R.[15] This suggests that Y_1R may be responsible in tumour proliferation, apoptosis, metastasis and angiogenesis.[16]

With Y_1R being a potential drug target, traceable high affinity Y_1R ligands are highly desirable tools for studying the localisation, regulation and function of this receptor. Lys^4(sCy5)-NPY was shown to be an agonist of Y_1R, Y_2R and Y_4R receptors, and of utility in the development of FACS-based functional assays of complex cell-based assay systems.[17] Another approach has been to derive fluorescent or radiolabelled analogues of the Y_1R arginamide antagonist series (BIBP3226, BIBO3304),[18] including pyridinium and cyanine based BIBP3226 derivatives suitable for fluorescent imaging.[19, 20]. An alternative starting point has made use of smaller NPY derived peptide ligands, such as the competitive Y_1R antagonist / Y_4R agonist BVD-15 (or BW1911U90), a nonapeptide modified from the NPY C-terminal fragment (

Figure 1).[21] This peptide has been amenable to conjugation with a variety of radiolabels and fluorophores. In particular, Guérin *et al*. showed that the Ile^4 residue could be substituted by

conjugated Lys to incorporate DOTA, NOTA or fluorine moieties,[22, 23] and we extended this result to include a rhodamine fluorophore.[24] No less notably, the Lys[4] substitution itself resulted in increased affinity,[23] and other basic residues were also well tolerated.[24] This prompted us to examine such analogues with Pro[3] as a point of conjugation and we have recently described propargyloxyproline containing Lys[4]- and Arg[4]-BVD-15 that could incorporate rhodamine B and 7-aminocoumarin fluorophores.[25] The tyrosine at the 5-position has been also shown to be capable of replacement with a conjugate group.[26]

Noting that the position and nature of the conjugated group and its linkage could have a significant influence on the pharmacology of the resulting peptide, here we have examined the 2- and 4-position as the points of conjugation, and identified a number of potent novel fluorescently labelled Y_1R-targeting peptidic ligands. We have explored the utility of one of these and found it to be an excellent reagent for performing fluorescent imaging of recombinant cells transfected with Y_1R or Y_4R, allowing the development of receptor binding studies in intact living cells.

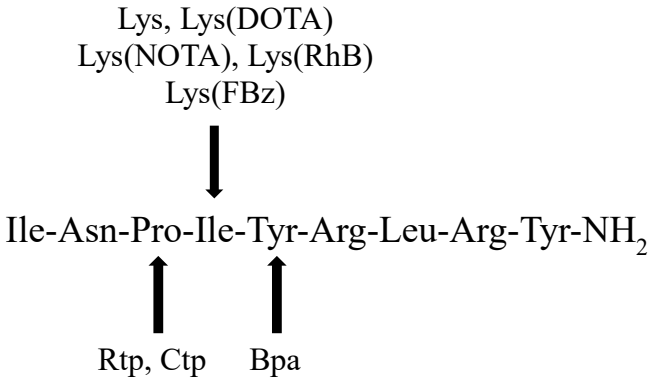

Figure 1: The amino acid sequence of BVD-15 scaffold and reported conjugated amino acid replacements. FBz = 4-fluorobenzoyl, Rtp = rhodamine B-triazolyl-proline, Ctp = coumarin-triazolyl-proline, Bpa = 4-benzoylphenylalanine.

Results and Discussion

Chemistry

We began by expanding our pool of conjugate precursors to include a variety of rhodamine B (RhB) conjugates (**Figure 2**), taking advantage of the capacity to generate different linkers from a common, inexpensive precursor,[27] as well as two cyanine dyes (**Figure 2**) Cy5.5 and sulfo-Cy5 (sCy5). We extended the types of conjugates included at Lys^4, but also encompassed substitutions at Asn^2. While a lysine residue at the 2-position had been shown to be detrimental to Y_1R activity,[23] the influence on subsequent conjugation had not been tested.

The synthesis of the conjugated BVD-15 analogues was achieved by one of three distinct methods. While all peptide backbones were prepared by adapting standard Fmoc-based solid phase peptide synthesis (SPPS) strategy, both solid and solution phase side-chain labelling were attempted. To facilitate chemoselective derivatisation at the 2-position, the 4-position was substituted by an Arg residue, which retains high affinity for Y_1R receptors.[25]

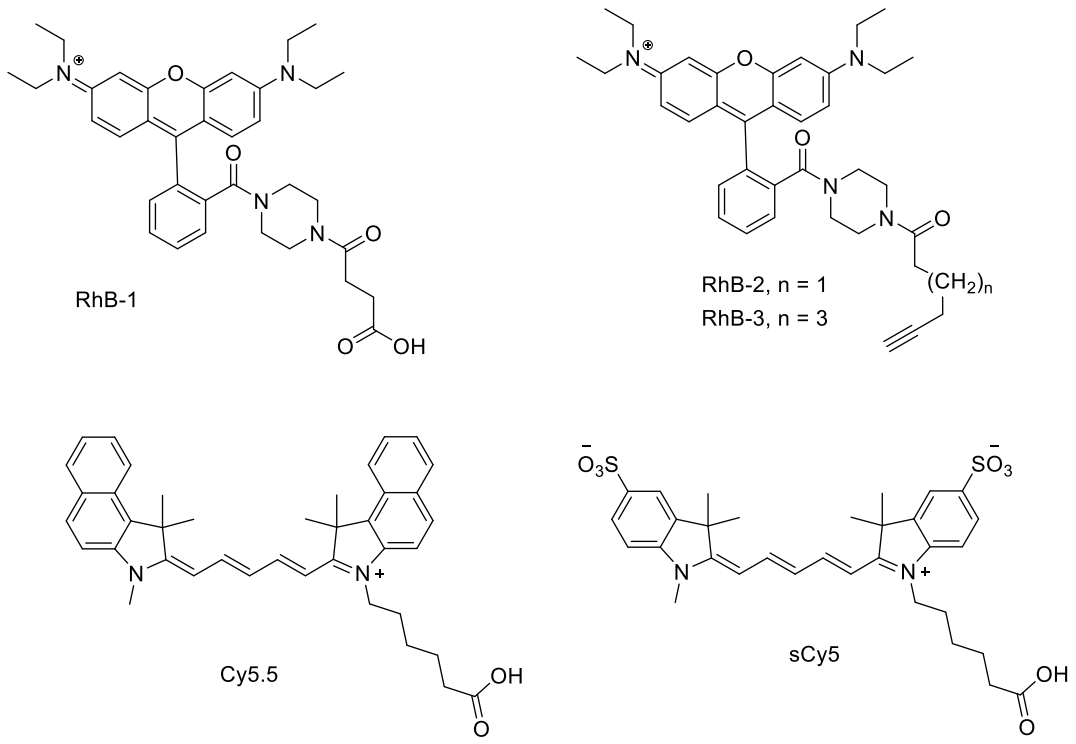

Figure 2: Fluorescent dye conjugates utilised in this study.

In the first instance, linear peptides were synthesised with N-terminal Fmoc protection and amide coupling in solution was achieved using carboxyl-functionalised fluorophores, followed by Fmoc-deprotection to yield the target peptides (analogues **A**, **D**, **F** and **H**, using Method 1 in **Scheme 1**. In Method 2, selective ε-amine modification on solid phase was achieved by incorporating ε-Mtt-protected Lys as an orthogonal protection. The Mtt group was selectively cleaved off by treating with 25% HFIP and 5% TIPS, and then the Cy5.5 fluorophore was coupled as an N-succinimidyl ester. The N-terminal Fmoc group was removed by 20% piperidine prior to the final acidolytic cleavage, giving analogues **E** and **G**. In order to prepare analogues **B** and **C** where conjugates are linked by the 1,2,3-triazole group, Fmoc-Lys(azide)-OH was incorporated at the 4-position. Labelling was then achieved by solution phase CuAAC reaction using the alkyne-containing RhB-2 and RhB-3, in presence of $CuSO_4$ and sodium ascorbate as the catalysts (Method 3).[25] The synthesised analogues with their analytical data are summarised in **Table 1**.

Method 1

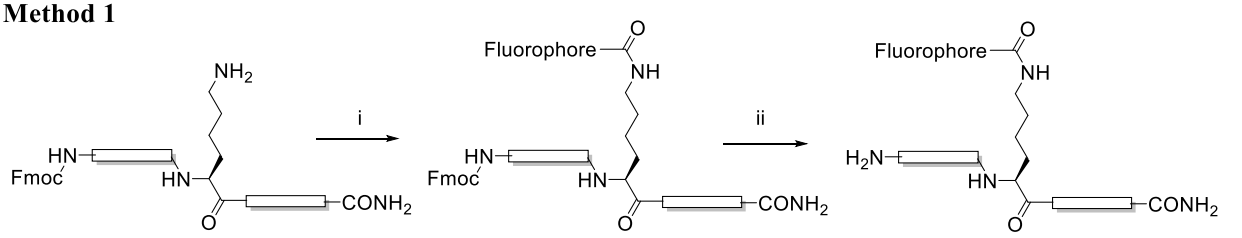

Method 2

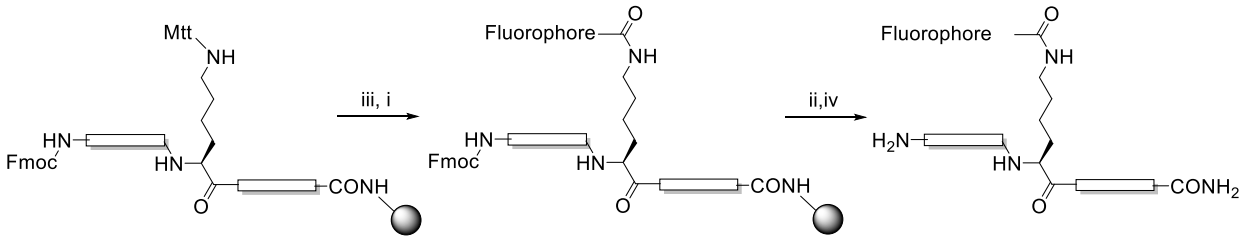

Method 3

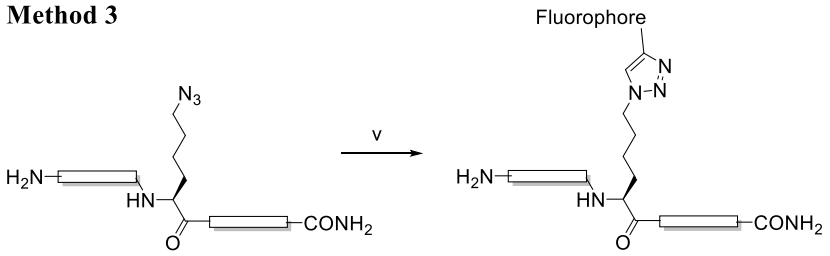

Scheme 1: Fluorescent labelling of BVD-15 analogues. Reagents and Conditions: i. fluorophore-COOH (1.2 *eq.*), PyClock (2 *eq.*), NMM (12 *eq.*), DMF, overnight (Note that for **E** and **G**, Cy5.5, was coupled as an N-succinimidyl ester); ii. Piperidine (20%) in DMF, 5 min×2; iii. HFIP (25%) and TIPS (5%) in DCM, 30 min; iv. TFA-TIPS-DMB (92.5%:2.5%:5%), 3 h; v. RhB-alkyne (2 *eq.*), $CuSO_4$ (0.5 *eq.*), THPTA (2.5 *eq.*), aminoguanidine (25 *eq.*), sodium ascorbate (25 *eq.*), DMSO 2% in potassium phosphate buffer (0.1 M, *pH* = 7.4), 1 h.

Table 1: Fluorescently labelled BVD-15 analogues and their analytical data

Code	Sequence	Labelling Method	MW (Calc.)	ESI-MS m/z [a]	LC/MS RT. (min) [b]	HPLC purity (%)
A	INPK(RhB-1)YRLRY-NH_2	1	1815.2	605.9	10.24[c]	93
B	INP(K-N_3-RhB-2)YRLRY-NH_2	3	1839.3	613.9	13.42	99
C	INP(K-N_3-RhB-3)YRLRY-NH_2	3	1867.3	623.3	13.58	99
D	IK(RhB-1)PRYRLRY-NH_2	1	1857.3	620.1	13.09	99
E	INPK(Cy5.5)YRLRY-NH_2	2	1786.5	596.6	14.12[d]	94
F	INPK(sCy5)YRLRY-NH_2	1	1859.3	621.2	12.72	98
G	IK(Cy5.5)PRYRLRY-NH_2	2	1829.3	610.6	14.11[d]	99
H	IK(sCy5)PRYRLRY-NH_2	1	1901.3	635.4	12.06	98

a. ESI-MS base peak corresponds to $[M+3H]^{3+}$.
b. HPLC retention time using a Phenomenex Luna C-8 column (100Å, 3µm, 100×2.00mm). The gradient is composed of 100% H_2O (0.1% TFA) for 4 min, 0-60% acetonitrile in H_2O (0.1% TFA) over 10 min, and isocratic 60% acetonitrile in H_2O (0.1% TFA) for 1 min. Detection wavelength = 214 nm.
c. For analogue **A**, the gradient is composed of 100% H_2O (0.1% TFA) for 4 min, 20-100% acetonitrile in H_2O (0.1% TFA) over 10 min, and isocratic 100% acetonitrile (0.1% TFA) for 1 min.
d. For analogue **E** and **G**, the gradient is composed of 100% H_2O (0.1% TFA) for 4 min, 0-80% acetonitrile in H_2O (0.1% TFA) over 10 min, and isocratic 80% acetonitrile (0.1% TFA) for 1 min.

Pharmacological analysis of NPY analogues

We examined the functional properties of the BVD-15 analogues as antagonists of NPY-induced Y_1R engagement with β-arrestin2, a GPCR effector protein involved in G protein independent signalling and agonist induced receptor desensitisation and internalisation.[28] This assay gives a strong functional readout consistent with other second messenger assays, and the limited receptor reserve allows discrimination of agonist efficacy via changes in R_{max} as compared to standard second messenger assays.[20, 21, 28-30] Unlabelled [Lys^4]BVD-15 [23, 24] behaved as a competitive reversible antagonist of NPY stimulated responses, as indicated by Schild analysis (**Figure 3A**) with a pA_2 of 7.5, and all but one of the labelled ligands showed comparable high affinity antagonism. pK_b values were calculated from NPY concentration response curve shifts in the presence of a single antagonist concentration (100 nM or 300 nM; **Figure S1**), and ranged from 6.9 to 7.9 with the rhodamine-linked triazole compound **B**

showing highest affinity (**Table 2**). Of the four cyanine labelled derivatives, three were antagonists (**Table 2**) with compound **H** [Lys^2(sCy5), Arg^4]BVD-15 showed highest affinity, and shared the surmountable antagonist characteristics of [Lys^4]BVD15 (**Figure 3B**). Interestingly, substitution of the sCy5 fluorophore for Cy5.5 at the same 2-position led to compound **G** showing partial agonism in the Y_1R arrestin recruitment assay, with a pEC_{50} of 7.04 ± 0.19 and a maximal response of 52.8 ± 4.8% compared to that elicited by 1 µM NPY (n = 3; **Figure S2**). In contrast, analogues **E**, **F** (both cyanine labelled at 4-position) and **H** showed no agonism at concentrations up to 1 µM.

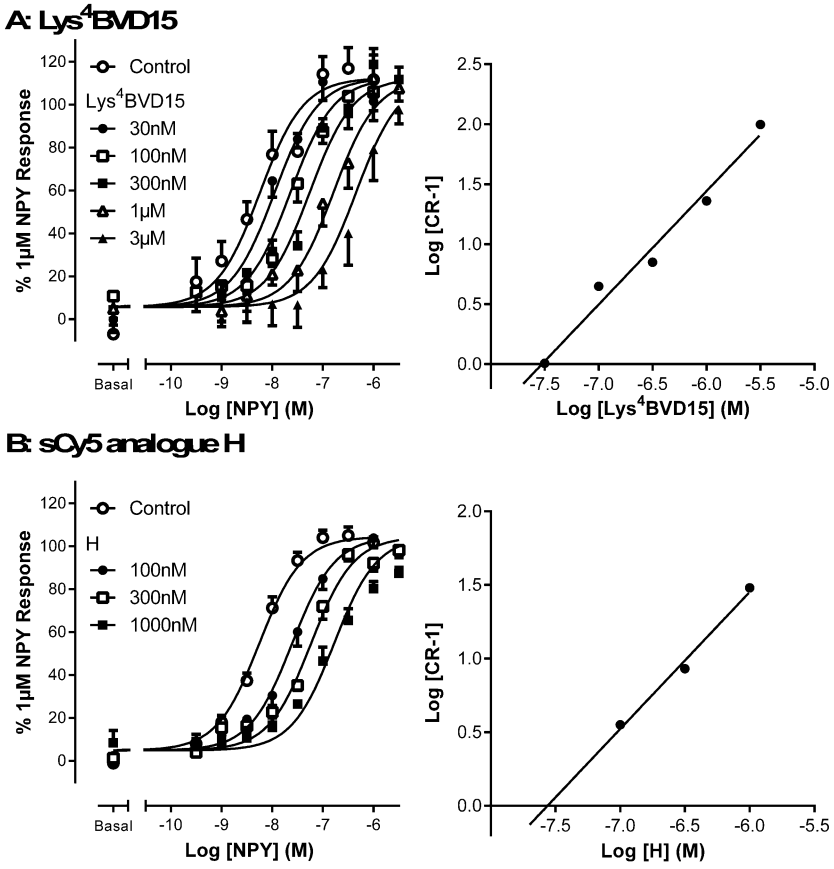

Figure 3: Surmountable antagonism of NPY stimulated Y_1R activation by unlabeled [Lys^4]BVD15 (Panel A) and sCy5-labelled derivative **H** (Panel B). Stably transfected HEK293 Y_1R-β-arrestin2 cells were pretreated for 30 min with the antagonist peptide at the indicated concentrations, prior to 1 h NPY stimulation. β-arrestin2 recruitment was quantified by high content imaging complementation assay as described in materials and methods. Pooled data from 5 (**A**) or 4-7 experiments (**B**), globally fitted to obtain NPY pEC_{50} estimates, were used for Schild analysis in the right hand panels. These derived pA_2 affinity

estimates of 7.53 (analogue **A**) and 7.56 (analogue **H**) and respective slopes of 0.95 and 0.93, indicative of competitive reversible antagonism.

Table 2: Affinity estimates for BVD-15 analogues derived from functional measurements or [^{125}I]PYY competition binding.

Code	Sequence	pK_b	pK_i (±SEM)
[Lys^4]BVD-15 [24]	INPKYRLRY-NH_2	7.5±0.1	8.6±0.1
A	INPK(RhB-1)YRLRY-NH_2	7.6±0.2	9.5±0.2
B	INP(K-N_3-RhB-2)YRLRY-NH_2	7.9±0.2	9.6±0.1
C	INP(K-N_3-RhB-3)YRLRY-NH_2	7.6±0.2	9.4±0.1
D	IK(RhB-1)PRYRLRY-NH_2	6.9±0.4	9.2±0.1
E	INPK(Cy5.5)YRLRY-NH_2	7.3±0.1	8.4±0.2
F	INPK(sCy5)YRLRY-NH_2	7.3±0.1	N.D.
G	IK(Cy5.5)PRYRLRY-NH_2	agonist*	8.8±0.3
H	IK(sCy5)PRYRLRY-NH_2	7.5±0.2	9.4±0.1

* pEC_{50} = 7.0 ± 0.2, partial agonist (**Figure S2**).
N.D. = not determined
pK_b estimates derived from pooled data using the Y_1R-β-arrestin2 recruitment assay presented in **Figure S1** (n = 4 or greater). For comparison, pK_i estimates (n = 3, except compound **B** n =2) are derived from [^{125}I]PYY binding studies in Y_1R-GFP membranes, performed under low sodium conditions in the absence of guanine nucleotides.

We screened the fluorescent BVD-15 analogues for their ability to specifically label 293TR cells stably expressing the GFP-tagged Y_1R. In plate-reader based imaging assays, RhB labelled derivatives (e.g. **A**, **Figure 4**) exhibited specific Y_1R receptor binding, predominantly localised to the plasma membrane that was inhibited by NPY and the non-peptide Y_1R antagonist BIBO3304. Cy5.5 analogues (**E**, **G**) displayed significant non-specific binding in addition to cellular labelling and were not pursued further. However, compound **H** displayed specific plasma membrane labelling of Y_1R-GFP cells at concentrations as low as 1 nM (**Figure 5A**), and specific binding was fully inhibited by unlabelled competitors such as NPY or BIBO3304.

Peptide **H** was therefore chosen to develop a plate-reader imaging based Y_1R binding assay, using living whole cells. Peptide **H** displayed fluorescence consistent with the sCy5 labelling, with excitation and emission maxima at 653 nm and 667 nm respectively, and a relative quantum yield of 127% compared to sCy5-NHS alone (Supplementary Fig. 4). Based on optimised incubation conditions of 30 min at 37°C, saturation analysis demonstrated one site

binding and derived a Y_1R pK_D for **H** of 7.16 ± 0.06 (n = 4) (**Figure 5B**), an estimate of affinity that was not significantly different from the pK_b derived by functional analysis (**Figure 3**). Furthermore, initial BIBO3304 competition data compared a family of curves at different **H** concentrations (1 nM, 10 nM and 100 nM), yielding BIBO3304 pIC_{50} values of 9.06 ± 0.07, 8.69 ± 0.07 and 8.31 ± 0.07 respectively (n = 4, **Figure 5B**). The proportionate shift in competing ligand IC_{50} was consistent with equilibrium conditions and the Cheng-Prusoff relationship. Additional affinity estimates for BIBO3304 (pK_i = 8.9) and **H** (pK_i = 7.3) determined by this method were consistent with our other whole cell data.

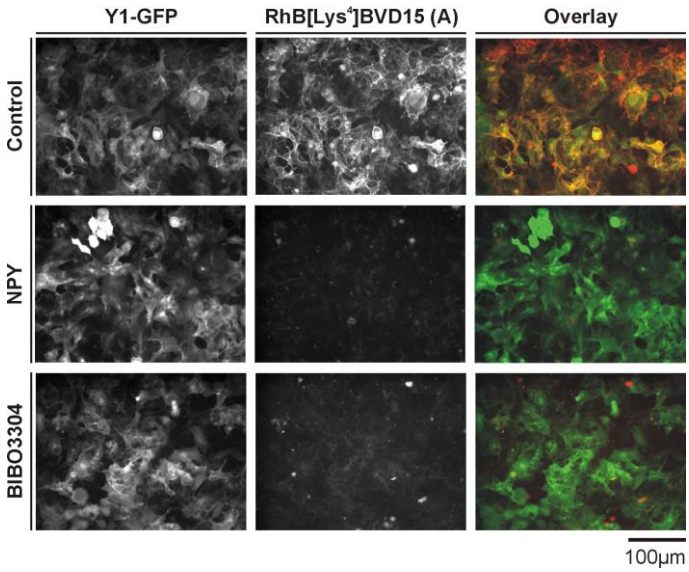

Figure 4: Cellular labelling of Y_1R-GFP by [Lys^4(RhB)]BVD-15 (**A**). 293TR Y_1R-GFP cells were incubated for 30 min at 37ºC with 10 nM **A** in the absence (control) or presence of 100 nM NPY or 100 nM BIBO3304. Representative IX Micro images (from one of 3 experiments) of GFP (left) or RhB fluorescence (centre) are indicated, demonstrating extensive cell surface labelling using ligand **A** and co-localisation with the GFP-tagged Y_1R.

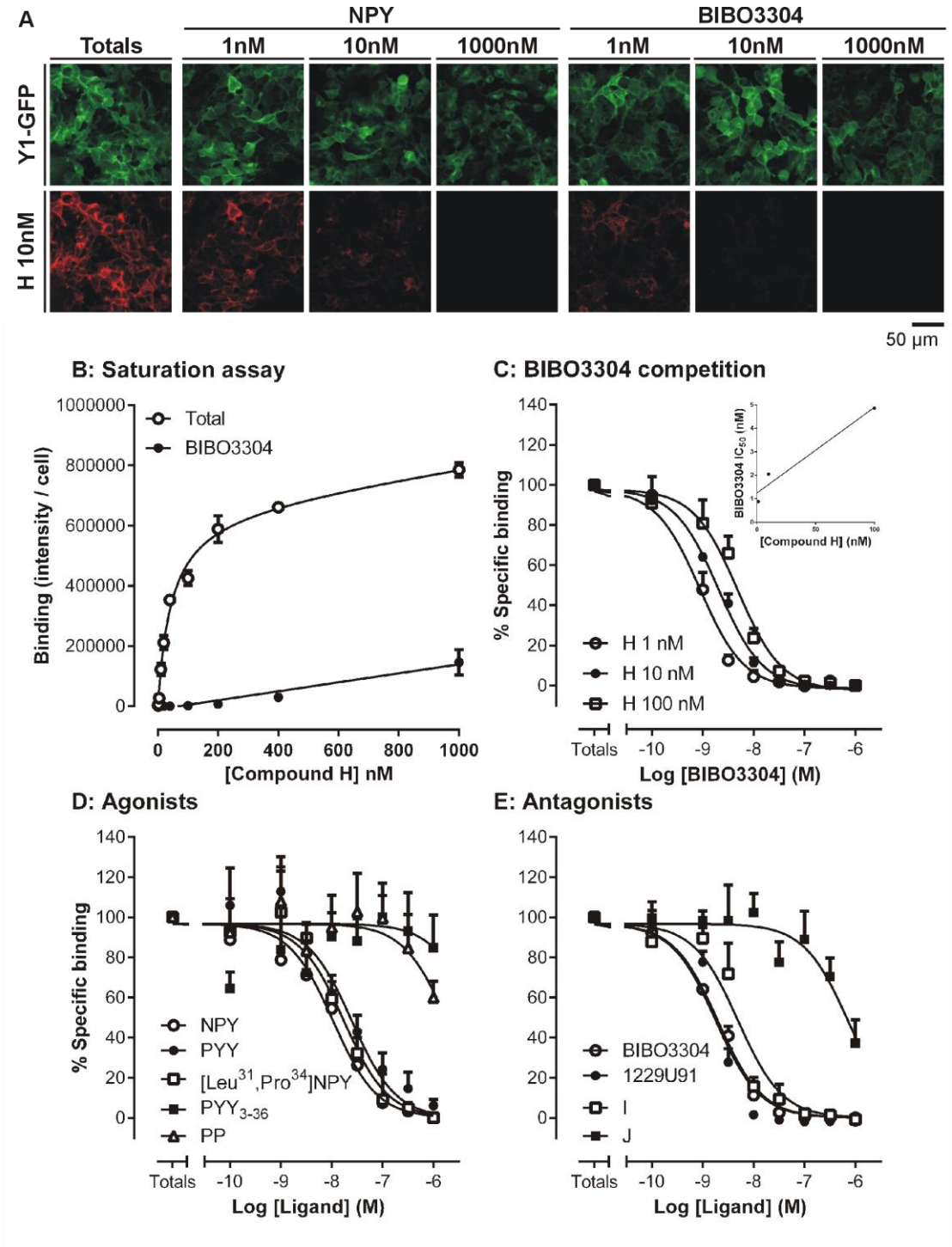

Figure 5: Y_1R binding assays using sCy5 labelled analogue **H**. Images from the IX Ultra platereader (Panel A, 400×400 pixels from original 1000×1000 acquisition) show binding of 10 nM **H** (red channel) to live 293TR Y_1R-GFP cells in the absence or presence of different NPY or BIBO3304 concentrations (30 min, with Y_1R-GFP images (green) also presented for comparison. Saturation analysis (Panel B) was performed in the absence (Total) or presence of 1 µM BIBO3304 (example experiment representative of 4). Pooled competition binding data (Panel C-E, at least 3 experiments) were derived from granularity analysis of the ligand images, normalised to total specific binding (100%). In C, BIBO3304 competition curves were performed at three **H** concentrations; the plot of the BIBO3304 IC_{50} versus ligand concentration (inset) provides additional Ki affinity estimates for both BIBO3304 and **H** quoted in text (see Materials and Methods). pKi estimates were also obtained for a range of agonist peptides (Panel D) and antagonists (Panel E), as indicated in **Table 4**.

Peptide H was employed in the study of a range of known Y receptor agonists, antagonists as well as a series of analogues prepared in related studies (**Table 3**).[29, 31] The expected Y_1-like pharmacology in the competition assay was observed for agonist peptides (Figure 5D; NPY = [Leu31, Pro34]NPY ≥ PYY > PYY3-36 = PP), as previously described for many Y_1 receptor systems,[32] and also antagonists, such as the dimeric peptide 1229U91.[29] The order of affinity based on pKi values from these experiments was consistent with [125I]PYY binding assays for representative ligands performed in Y1R-GFP cell membranes (and previously described data from Y_2Y_4 receptor knockout mice).[29] For the non-peptide antagonist BIBO3304 there was good correspondence between affinities measured in these formats, and also functional measurements previously reported.[28] For the peptide ligands the actual pK_i values for the whole cell assays were consistently lower than for membrane based assays (**Table 4**). The reason for this discrepancy is not obvious, but note that there is a closer correlation between the competition binding (pK_i) and the functional antagonism in the whole cell system. The difference may be due to the buffer conditions in routine Y receptor membrane binding assays (low sodium and absence of guanine nucleotides) that are designed to promote the high affinity ternary receptor complex, and maximize radiolabelled agonist peptide binding.[33] The non-physiological buffer cation concentrations might also directly affect peptide ligand binding to the receptor. Thus one of the important advantages of our measurements using fluorescent antagonist binding to whole cells, in physiological buffer, is that the affinities obtained should closely correspond to observations from functional data, particularly for agonists. Indeed the

estimates of agonist affinity by this route (

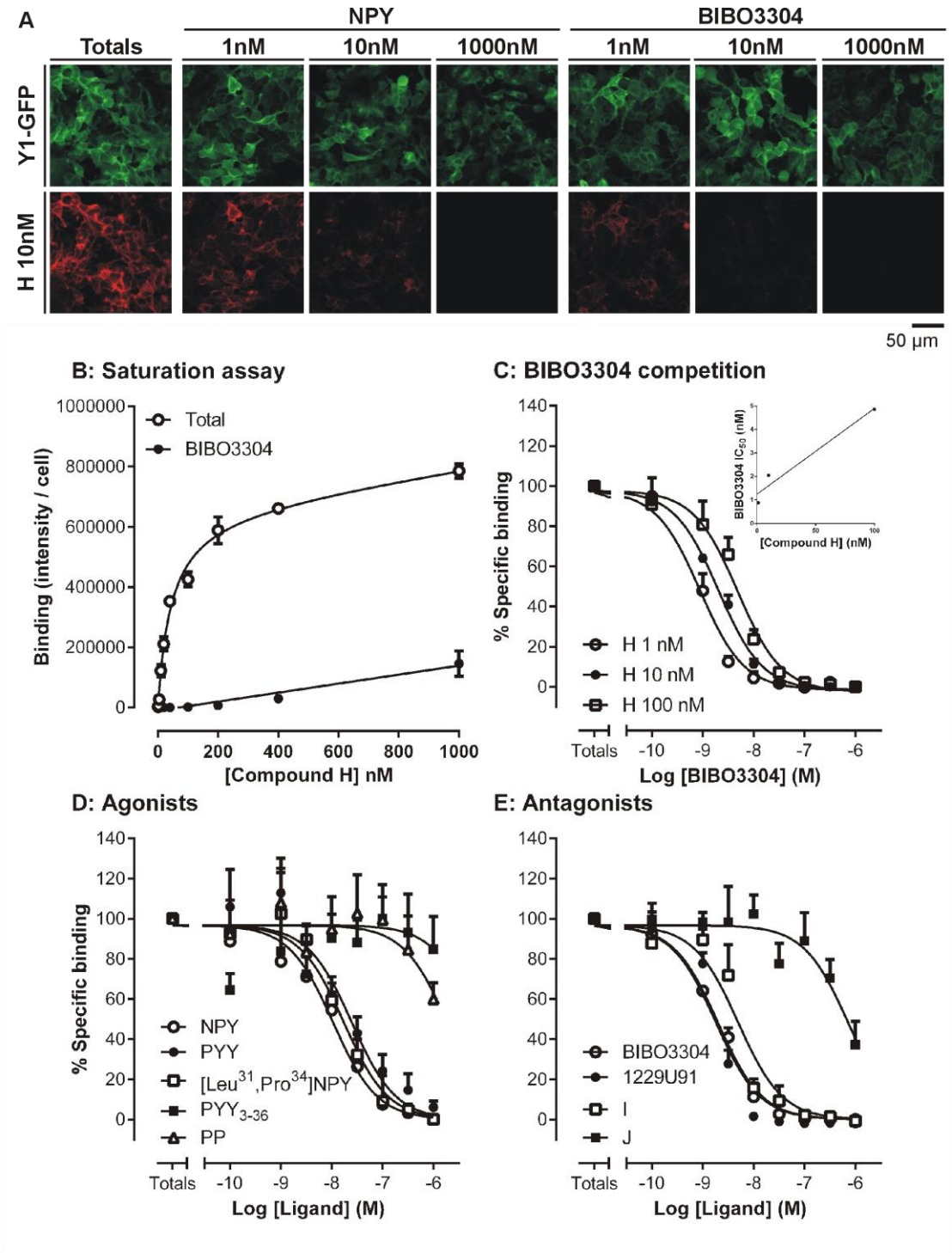

Figure 5**D**) do closely correspond with their potencies in Y_1R-arrestin recruitment assay previously reported,[28] as anticipated for a response with limited receptor reserve.[33] We also assayed compounds for which we had membrane competition binding data spanning a range

of affinities, including analogues of 1229U91, **I** and **J** (**Figure 5E**; **Table 3**)[29] and some unlabeled BVD-15 analogues **K** – **N** (**Table 3**) and found the same trends (**Table 4**, **Figure S3**).

Table 3: Analytical data of dimeric 1229U91 analogues and other unlabelled BVD-15 analogues.

Code	Sequence	MW (Calc.)	ESI-MS m/z	LC/MS RT. (min)[c]	HPLC purity (%)	Ref.
I	Bis(Lys[4])1229U91	2436.9	851.6[a]	11.16	98	[29]
J	Bis(des-Ile[1])1229U91	2126.4	748.1[a]	11.00	99	[29]
K	FBz-INPKYRLRY-NH_2	1343.6	672.8[b]	12.30	97	
L	INPOYRLRY-NH_2	1207.4	604.7[b]	10.55	98	[24]
M	FBz-INPRF*RLRY-NH_2	1506.7	754.2[b]	12.93	99	
N	INPRF*RLRY-NH_2	1384.6	693.2[b]	11.51	98	

a. ESI-MS base peak corresponds to $[M+TFA+3H]^{3+}$. Note that $[M+3H]^{3+}$ peaks were observed at lower intensity.
b. ESI-MS base peak corresponds to $[M+2H]^{2+}$.
c. HPLC retention time using a Phenomenex Luna C-8 column (100Å, 3µm, 100×2.00mm). The gradient is composed of 100% H_2O (0.1% TFA) for 4 min, 0-60% acetonitrile in H_2O (0.1% TFA) over 10 min, and isocratic 60% acetonitrile in H_2O (0.1% TFA) for 1 min. Detection wavelength = 214 nm.

FBz = 4-fluorobenzoyl, O = ornithine, F* = Phe(4-CH_2NH-FBz).

Table 4: Competition binding assays at Y_1R and Y_4R using compound **H** as a competing ligand, in comparison to radioligand binding data.

Peptide	Y_1R (pKi)[a] Live cell imaging (H)	Y_1R (pK_i) [^{125}I]PYY membranes	Y_4R (pKi) [a] Live cell imaging (H)	Y_4R (pK_i) [^{125}I]PP membranes
NPY	7.95 ± 0.12	9.75 ± 0.16	-	-
PYY	7.67 ± 0.10	9.50 ± 0.23	-	-
Leu[31],Pro[34]-NPY	7.82 ± 0.11	-	-	-
PYY(3-36)	< 6.0	-	-	-
PP	< 6.0	-	8.69 ± 0.11	10.1 ± 0.21[34]
BIBO3304	8.76 ± 0.04	9.25 ± 0.11	-	-
1229U91	8.80 ± 0.07	9.90 ± 0.06	7.21 ± 0.10	9.6 ± 0.11[34]
I	8.35 ± 0.12	10.18 ± 0.12	7.20 ± 0.10	-
J	6.03 ± 0.59	8.91 ± 0.08	6.91 ± 0.11	-
K	6.48 ± 0.17	9.10 ± 0.08	-	-
L	7.69 ± 0.09	9.73 ± 0.01	-	-
M	6.23 ± 0.11	8.62 ± 0.19	-	-
N	7.59 ± 0.10	9.74 ± 0.08	-	-

[a] pKi estimates from n = 3-4 whole cell competition binding (**H**) in Y_1R-GFP or Y_4R-GFP cells, using the Cheng-Prusoff correction based on **H** pK_D derived from saturation analysis in imaging studies. pK_i estimates derived from [^{125}I]PYY binding to 293TR Y_1R-GFP membranes (n = 2-6)

Compound **H** displayed moderate affinity for Y_4R (**Figure 6**), with saturation binding assays yielding a pK_D for **H** of 6.26 ± 0.11 (n = 4), 8 fold lower than for Y_1R. It did not bind cells expressing Y_2R or Y_5R (data not shown) at up to 1 µM, as might be predicted from the reported

selectivity profile for BVD-15.[35] In contrast to its actions at the Y_1R, **H** was a Y_4R partial agonist, a property shared by BVD-15, in the β-arrestin2 recruitment assay (**Figure 6**; pEC_{50} = 7.10 ± 0.19, 1 μM response 59.0 ± 3.6 %, 100 nM PP, n = 6); other cyanine BVD-15 analogues **E-G** displayed limited Y_4R agonism at the highest concentration tested (1 μM). At 100 nM, **H** selectively labelled 293TR cells expressing Y_4R-GFP (**Figure 6A**), enabling competition binding studies to derive pKi estimates for human PP, 1229U91 and its analogues **I** and **J** (**Figure 6C**; **Table 4**). As previously discussed, these estimates were lower than those previously reported for [^{125}I]PP agonist binding studies in Y_4R containing membranes.[34] However, the estimates of PP and 1229U91 affinity in whole cells by this route closely corresponded with their potencies in the arrestin recruitment assay (PP pEC_{50} = 8.77 ± 0.07, n = 5; 1229U91 weak partial agonist pEC_{50} = 7.43 ± 0.41, n = 4; **Figure 6D**). Comparisons of Y_1R/Y_4R binding affinities of 1229U91 analogues demonstrated that **I** had equivalent Y_1R/Y_4R selectivity as 1229U91 (16-30 fold selective for Y_1R), while removal of the terminal Ile residues in **J**, reversed the selectivity profile between these subtypes (approximately 8 fold higher affinity for Y_4R over Y_1R).

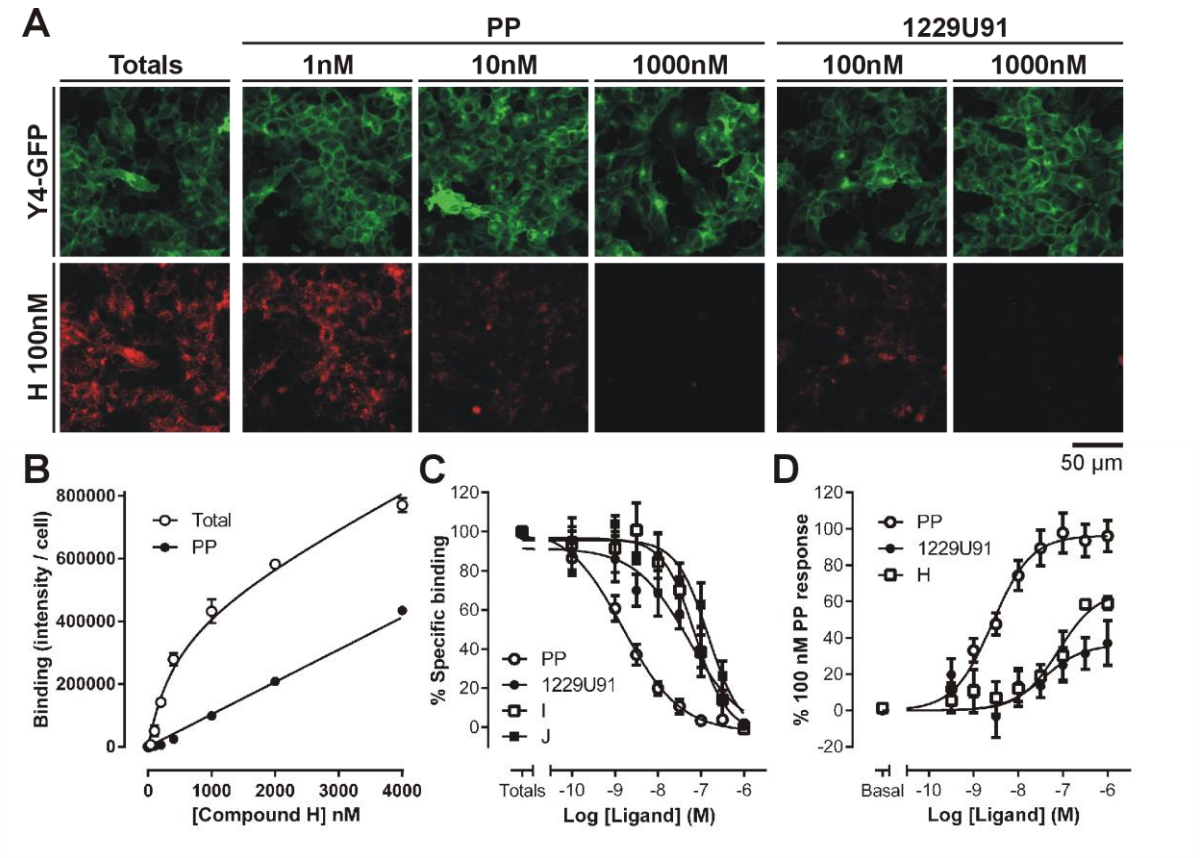

Figure 6: [Lys[2](sCy5), Arg[4]]BVD-15 (**H**) is also a Y_4R fluorescent ligand. Panel A illustrates representative images of 100 nM **H** binding (red) to 293TR Y_4R-GFP cells (green) in the absence or presence of the endogenous peptide PP or 1229U91. Quantification of these data obtained saturation data for **H** (pK_D 6.26), in which non-specific binding was assessed in the presence of 1 µM PP (Panel B, experiment representative of 4), and competition curves in Panel C (pooled from 4-7 experiments), from which the pKi estimates in **Table 4** were determined. In the Y_4R-β-arrestin2 recruitment assay (Panel D), **H** was a partial agonist compared to PP, but of higher relative efficacy than 1229U91 (pooled data 4-10 experiments).

In summary, our studies of fluorescent labelling of the BVD-15 scaffold has allowed us to identify some new features of the peptides structure-activity relationships. First, we confirmed the general tolerance for modification at the 4-position, with retention of antagonistic activity at levels similar to the parent peptide in the presence of rhodamine derivatives and cyanine dyes. Second, we showed for the first time that the Asn residue at 2-position, in combination with introduction of an Arg at 4-position yields peptides with retained affinity. However, while the sulfated Cy5 (sCy5) ligand is an antagonist, the more hydrophobic Cy5.5 label has agonist properties. This is significant as only one other example of a truncated NPY analogue has been shown to be an agonist.[26] We have also shown that analogue **H** is an excellent ligand for performing receptor binding studies at Y_1R in intact cells using high content imaging, with low

levels of non-specific binding. Finally, we also show that analogue **H** has Y_4R agonism, albeit at a lower level of affinity compared to Y_1R binding. Thus analogue **H** is also a suitable ligand for conducting competition binding and functional assays against Y_4R and has been applied recently in structure-activity studies of the dimeric Y_4 agonist, BVD-74D [36, 37]. The ready synthesis of this fluorescent ligand and its favourable properties will be of great utility in the development of new ligands for these two important receptors.

Experimental Methods

Material

N^{α}-Fmoc protected amino acids were purchased from Auspep, Chemimpex and Mimotopes. Rink amide resin (0.53 meq/g, 100-200 mesh), HCTU and PyClock were obtained from Chemimpex. TFA, TIPS, DMB, HFIP, DIPEA, piperidine, $CuSO_4$, aminoguanidine, sodium ascorbate and DMSO were purchased from Sigma-Aldrich. All solvents were obtained from Merck. Cyanine dyes were purchased from Lumiprobe and W&J PharmaChem. THPTA was a gift from Dr Bim Graham's group (Monash Institute of Pharmaceutical Sciences, Monash University). The Rhodamine B derivatives were prepared in-house from the commercially available product (Sigma-Aldrich), according to Nguyen and Francis.[27] All solvents were of analytical grade, and all chemicals were used without further purification.

Molecular mass of peptides was determined by ESI-MS using a Shimadzu LCMS2020 instrument, incorporating a Phenomenex Luna C-8 column (100Å, 3μm, 100×2.00mm). Detection wavelength was set at 214 nm. This system used 0.05% TFA in MilliQ water as the aqueous buffer, and 0.05% TFA in acetonitrile as the organic buffer. The eluting profile was a linear gradient of 0-60% acetonitrile in water over 10 min at 0.2 ml/min.

Crude peptides were purified on a Phenomenex Luna C-8 column (100Å, 10μm, 250×21.2mm) utilising a Waters 600 semi-preparative RP-HPLC that incorporates a Waters 486 UV detector.

Detection wavelength was set at 230 nm. This system used 0.1% TFA in MilliQ water as the aqueous buffer, and 0.1% TFA in acetonitrile as the organic buffer. The eluting profile was a linear gradient of 0-80% acetonitrile in water over 60 min at 10 ml/min.

Peptide synthesis

General synthesis

Linear peptides (0.1 mmol scale) were synthesised on Rink amide resin using a 3-channel serial automated peptide synthesiser ("PS3", Protein Technologies Inc.), which adopted standard Fmoc-based solid phase synthesis strategy. Fmoc deprotection was performed by piperidine (20% v/v) in DMF for 2×5 min. Fmoc protected amino acids (3 *eq.*) were coupled using DMF as solvent, and DIPEA in DMF (7% v/v) with HCTU (3 *eq.*) as the activating agent for 50 min.

Protected peptidyl-resins were cleaved by treating with a cocktail (5 ml) composed of TFA-TIPS-DMB (92.5%:2.5%:5%) for 3 h. The cleavage mixture was then filtered, concentrated by stream of N_2, precipitated in cold Et_2O and centrifuged at 3000 rpm for 5 min. The crude product was dissolved in water-acetonitrile mixture (50%:50%) and lyophilised.

Labelling methods

Method 1: The N^{α}-Fmoc protected linear peptide dissolved in DMF (0.6 ml) was treated with carboxyl-functionalised fluorophore of interest (1.2 *eq.*), PyClock (2 *eq.*) and NMM (12 *eq.*) overnight. After DMF was removed *in vacuo*, the product was washed by TFA (1 ml), precipitated by cold Et_2O and centrifuged at 3000 rpm for 5 min. The N^{α}-Fmoc group was then removed by piperidine (20%) in DMF (5 ml) for 30 min and the reagents were evaporated *in vacuo*. The product was re-dissolved in water-acetonitrile (50%:50%) and lyophilised.

Method 2: The protected peptidyl-resin containing a Lys(Mtt) residue was treated with HFIP (25%) and TIPS (5%) in DCM (5 ml) for 30 min to selectively remove the Mtt group. Cy5.5

(as an N-succinimidyl ester) was conjugated by treating overnight in an alkaline condition created by DIPEA (10 *eq.*).

Method 3: Linear peptide containing a Lys(azide) residue (15 mg) was labelled by treating with a mixture of RhB-alkyne (2 *eq.*), $CuSO_4$ (0.5 *eq.*), THPTA (2.5 *eq.*), sodium ascorbate (25 *eq.*) and aminoguanidine (25 *eq.*) in a potassium phosphate buffer containing 2% DMSO, where the final concentration of linear peptide was 0.2 mM. The mixture was stirred for 1 h and lyophilised.

Peptides were purified by RP-HPLC as described above. The purity of all peptides are ≥ 93% according to the HPLC chromatographs produced by the ESI-MS method described above, and MS data corresponded to the expected m/z values. Additional details are provided in Table 1, Table 3 and Supporting Information.

Cell culture

HEK293T and 293TR cells (Invitrogen) were cultured in Dulbecco's modified Eagle's medium (DMEM, Sigma-Aldrich) supplemented with 10% foetal bovine serum, 293TR cell lines inducibly expressing Y_1R or Y_4R tagged with C-terminal GFP, and dual HEK293 cells co-expressing Y receptor-Yc and β-arrestin2-Yn (where Yc and Yn are complementary fragments of YFP) are as previously reported.[28, 38]

[^{125}I]PYY competition binding studies in membranes

Competition binding assays were carried out as described previously.[28, 38] Using membranes from the 293TR Y_1R-GFP cells, competition binding assays were performed for 90 min at 21°C in buffer (25 mM HEPES, 2.5 mM $CaCl_2$, 1.0 mM $MgCl_2$, 0.1 % bovine serum albumin, 0.1 mg/ml bacitracin; *pH* = 7.4), increasing concentrations of unlabelled ligands (10^{-12} M to 10^{-6} M, duplicate) and [^{125}I]PYY (15 pM). Non-specific binding in these experiments comprised less than 5% of total counts, and was subtracted from the data.

In both sets of data, IC_{50} values were calculated from displacement curves (repeated 2-3 times for each peptide, fitted using non-linear least squares regression in GraphPad Prism v6 (GraphPad software, San Diego CA, U.S.A). They were converted to pK_i estimates using the Cheng-Prusoff relationship:

$$K_i = \frac{IC_{50}}{1 + {[RL]}/{K_{RL}}}$$

where [RL] and K_{RL} represent the concentration and equilibrium dissociation constant of [^{125}I]PYY respectively.

Y receptor-β-arrestin recruitment assays

Bimolecular fluorescence complementation (BiFC) based detection of Y receptor-β-arrestin2 association was performed as described previously.[28, 38]. The Y receptor arrestin BiFC cell lines

were seeded at 40,000 cells/well onto poly-D-lysine coated Greiner 655090 imaging plates, and experiments performed 24 hrs later. Stimulation with human NPY (Y_1R) or PP (Y_4R; Bachem, St. Helens, U.K.), or other ligands was performed in HEPES-buffered saline solution (HBSS) including 0.1% BSA (10^{-10} M-10^{-6} M) for 60 min at 37°C, with antagonist pre-incubations (30 min, 37°C) if required. Incubations were terminated by fixation with 3% paraformaldehyde in phosphate buffered saline (PBS, 10 min at 21°C), the cells were washed once with PBS and the cell nuclei were stained for 15 min with H33342 (2 µg/ml in PBS, Sigma). H33342 was then removed by a final PBS wash. Images (4 central sites/well) were acquired automatically on the IX Ultra confocal platereader, using 405 nm / 488 nm laser lines for H33342 and complemented YFP excitation respectively.

A granularity algorithm (MetaXpress 5.3) identified internal fluorescent compartments within these images of at least 3 µm diameter (range set to 3-12 µm), on the basis of granule intensity thresholds set with reference to the vehicle or positive plate controls (e.g. 1 µM NPY). The response for each data point (duplicate data) was quantified as mean granule average intensity/cell, normalised to the reference agonist response. Concentration response curves were fitted to the pooled data by non-linear least squares regression (GraphPad Prism), yielding estimates of agonist potency as pEC_{50} and maximum response (R_{max}). Where appropriate, the Gaddum equation was used to calculate an estimate of antagonist affinity:

$$pK_b = \log[CR - 1] - \log[B]$$

where CR is the concentration ratio (NPY EC_{50} in the presence of antagonist / control NPY EC_{50}), and [B] is the antagonist concentration used. To assess NPY concentration response curves in the absence and presence of multiple antagonist concentrations ([Lys^4]BVD-15 or compound **H**), Schild analysis was performed by global fitting of the curve families in GraphPad Prism; the Schild plot of $\log[CR - 1]$ versus log [B] illustrated the antagonist affinity estimate (pA_2) as the X-intercept of the fitted line.

Y receptor saturation and competition fluorescent ligand binding assays

293TR Y_1R-GFP or Y_4R-GFP cells were seeded at 20,000 cells / well in poly-D-lysine coated 96-well Greiner 655090 imaging plates, treated as required with 1 µg/ml tetracycline for 18-21 hrs and then used in experiments at confluence. Incubations were performed in HBSS/0.1% BSA, the permeable nuclear dye H33342 (2 µg/ml, Sigma) and competitor ligands as appropriate (10^{-10} M to 10^{-5} M) for 2 min, prior to the addition of fluorescent ligand at the concentration indicated. In saturation studies, non-specific binding was assessed in the presence of 1 µM BIBO3304 (Y_1R) or PP (Y_4R). After 30 min at 37°C the media was replaced with HBSS/0.1% BSA and plates were immediately imaged (2 sites/well). For cyanine analogues (e.g. **H**) an IX Ultra confocal platereader (Molecular Devices, Sunnyvale CA, U.S.A.) used laser excitation/emission filter settings appropriate for H33342 (DAPI), Y receptor-GFP (FITC), and fluorescent ligand (Cy5). For rhodamine B derivatives an IX Micro epifluorescence platereader (Molecular Devices) acquired the images using the TRITC excitation/emission filter set.

For fluorescent ligand binding using **H**, bound ligand fluorescence was quantified by granularity analysis (2-3 µm diameter granules; MetaXpress 5.3, Molecular Devices). Competition data were normalised to positive (totals 100 %) and negative (0%, in presence of either 1 µM NPY or 100 nM PP as appropriate) controls. For saturation studies, total and non-specific binding data were globally fitted using a one site binding model whereby:

$$\text{Total binding} = B_{max} \cdot \frac{[FL]}{[FL]+K_D} + NS \times [FL]$$

$$\text{Non-specific binding} = NS \times [FL]$$

[FL] is the fluorescent ligand concentration, B_{max} represents the maximum specific binding, NS is the gradient of the non-specific binding relationship and K_D is the equilibrium dissociation constant for compound **H**.

pIC_{50} values for unlabelled ligands were then determined from the pooled data using GraphPad Prism, and converted to pKi using the Cheng-Prusoff relationship described above and the fluorescent ligand K_D estimated from saturation data. In competition experiments in which compound **H** concentration [FL] in the assay was varied, the plot of BIBO3304 IC_{50} versus [FL] was fitted by linear regression using the relationship derived from the Cheng-Prusoff equation:

$$IC_{50} = \frac{K_i}{K_D} \times [FL] + K_i$$

The Y intercept for this fit derives an estimate of K_i for the competing ligand, BIBO3304, and the slope (K_i/K_D) also yields a further measurement of affinity of the fluorescent ligand **H** (K_D).

Glossary

DCM	Dichloromethane
DIPEA	N,N-diisopropylethylamine
DMB	1,3-dimethoxybenzene
DMF	N,N-dimethylformamide
HCTU	O-(1*H*-6-chlorobenzotriazol-1-y1)-N,N,N',N'-tetramethyluronium hexafluorophosphate
HFIP	Hexafluoroisopropanol
NMM	N-methylmorpholine
RhB	Rhodamine B
TFA	Trifluoroacetic acid
THPTA	Tris(3-hydroxypropyltriazolylmethyl)amine
TIPS	Triisopropylsilane

Supporting Information

Detailed synthesis procedures as well as additional supplementary figures showing dose-response curves for Y_1R binding by peptides, fluorescence excitation/emission spectra for compound **H** and HPLC profiles for synthesized peptides are provided on the Journal's website.

Acknowledgements

This work was supported by CRC for Biomedical Imaging Development (CRC-BID), Australia. ML was supported by an Australian Post-graduate Award scholarship. RRR was supported by the Nottingham-Monash PhD program.

References

(1) Tatemoto, K. (1982) Neuropeptide Y: Complete amino acid sequence of the brain peptide. *Proc. Natl. Acad. Sci. USA 79*, 5485-5489.

(2) Hoffmann, J. A., and Chance, R. E. (1983) Crystallization of bovine pancreatic polypeptide. *Biochem. Biophys. Res. Commun. 116*, 830-835.

(3) Tatemoto, K., and Mutt, V. (1980) Isolation of two novel candidate hormones using a chemical method for finding naturally occurring polypeptides. *Nature 285*, 417-418.

(4) Blomqvist, A. G., and Herzog, H. (1997) Y-receptor subtypes - how many more? *Trends. Neurosci. 20*, 294-298.

(5) Bromée, T., Sjödin, P., Fredriksson, R., Boswell, T., Larsson, T. A., Salaneck, E., Zoorob, R., Mohell, N., and Larhammar, D. (2006) Neuropeptide Y-family receptors Y_6 and Y_7 in chicken. *FEBS J. 273*, 2048-2063.

(6) Salaneck, E., Larsson, T. A., Larson, E. T., and Larhammar, D. (2008) Birth and death of neuropeptide Y receptor genes in relation to the teleost fish tetraploidization. *Gene 409*, 61-71.

(7) Kanatani, A., Mashiko, S., Murai, N., Sugimoto, N., Ito, J., Fukuroda, T., Fukami, T., Morin, N., MacNeil, D. J., Van der Ploeg, L. H. T., Saga, Y., Nishimura, S., and Ihara, M. (2000) Role of the Y_1 receptor in the regulation of neuropeptide Y-mediated feeding: comparison of wild-type, Y_1 receptor-deficient, and Y_5 receptor-deficient mice *Endocrin. 141*, 1011-1016.

(8) Kanatani, A., Ishihara, A., Asahi, S., Tanaka, T., Ozaki, S., and Ihara, M. (1996) Potent neuropeptide Y Y_1 receptor antagonist, 1229U91: blockade of neuropeptide Y-induced and physiological food intake. *Endocrin. 137*, 3177-3182.

(9) Thiele, T. E., Koh, M. T., and Pedrazzini, T. (2002) Voluntary alcohol consumption is controlled via the neuropeptide Y Y_1 receptor. *J. Neurosci. 22*, RC208.

(10) Thorsell, A. (2007) Neuropeptide Y (NPY) in alcohol intake and dependence. *Peptides 28*, 480-483.

(11) Nilsson, T., Cantera, L., and Edvinsson, L. (1996) Presence of neuropeptide Y Y_1 receptor mediating vasoconstriction in human cerebral arteries. *Neurosci. Lett. 204*, 145-148.

(12) Edvinsson, L., Ekblad, E., Håkanson, R., and Wahlestedt, C. (1984) Neuropeptide Y potentiates the effect of various vasoconstrictor agents on rabbit blood vessels. *Br. J. Pharmacol. 83*, 519-525.

(13) Desai, S. J., Borkar, C. D., Nakhate, K. T., Subhedar, N. K., and Kokare, D. M. (2014) Neuropeptide Y attenuates anxiety- and depression-like effects of cholecystokinin-4 in mice. *Neuroscience 277*, 818-830.

(14) Wahlestedt, C., Pich, E. M., Koob, G. F., Yee, F., and Heilig, M. (1993) Modulation of anxiety and neuropeptide Y-Y_1 receptors by antisense oligodeoxynucleotides. *Science 259*, 528-531.

(15) Reubi, J., Gugger, M., and Waser, B. (2002) Co-expressed peptide receptors in breast cancer as a molecular basis for in vivo multireceptor tumour targeting. *Eur. J. Nucl. Med. Mol. Imaging 29*, 855-862.

(16) Körner, M., and Reubi, J. C. (2006) Chapter 62 - Somatostatin and NPY, in *Handbook of Biologically Active Peptides* (Abba, J. K., Ed.) pp 435-441, Academic Press, Burlington.

(17) Schneider, E., Mayer, M., Ziemek, R., Li, L., Hutzler, C., Bernhardt, G., and Buschauer, A. (2006) A simple and powerful flow cytometric method for the simultaneous determination of multiple parameters at g protein-coupled receptor subtypes. *Chembiochem 7*, 1400-1409.

(18) Wieland, H. A., Engel, W., Eberlein, W., Rudolf, K., and Doods, H. N. (1998) Subtype selectivity of the novel nonpeptide neuropeptide Y Y1 receptor antagonist BIBO 3304 and its effect on feeding in rodents. *Br. J. Pharmacol. 125*, 549-555.

(19) Schneider, E., Keller, M., Brennauer, A., Hoefelschweiger, B. K., Gross, D., Wolfbeis, O. S., Bernhardt, G., and Buschauer, A. (2007) Synthesis and characterization of the first fluorescent nonpeptide NPY Y_1 receptor antagonist. *Chembiochem 8*, 1981-1988.

(20) Keller, M., Erdmann, D., Pop, N., Pluym, N., Teng, S., Bernhardt, G., and Buschauer, A. (2011) Red-fluorescent argininamide-type NPY Y1 receptor antagonists as pharmacological tools. *Biorg. Med. Chem. 19*, 2859-2878.

(21) Leban, J. J., Heyer, D., Landavazo, A., Matthews, J., Aulabaugh, A., and Daniels, A. J. (1995) Novel modified carboxy terminal fragments of neuropeptide Y with high affinity for Y_2-type receptors and potent functional antagonism at the Y_1-type receptor. *J. Med. Chem. 38*, 1150-1157.

(22) Guérin, B., Ait-Mohand, S., Tremblay, M.-C., Dumulon-Perreault, V. r., Fournier, P., and Bénard, F. (2009) Total solid-phase synthesis of NOTA-functionalized peptides for PET imaging. *Org. Lett. 12*, 280-283.

(23) Guérin, B., Dumulon-Perreault, V., Tremblay, M.-C., Ait-Mohand, S., Fournier, P., Dubuc, C., Authier, S., and Bénard, F. (2010) [Lys(DOTA)^4]BVD15, a novel and potent neuropeptide Y analog designed for Y_1 receptor-targeted breast tumor imaging. *Bioorg. Med. Chem. Lett. 20*, 950-953.

(24) Liu, M., Mountford, S. J., Zhang, L., Lee, I.-C., Herzog, H., and Thompson, P. E. (2013) Synthesis of BVD15 peptide analogues as models for radioligands in tumour imaging. *Int. J. Pept. Res. Ther. 19*, 33-41.

(25) Northfield, S. E., Mountford, S. J., Wielens, J., Liu, M., Zhang, L., Herzog, H., Holliday, N. D., Scanlon, M. J., Parker, M. W., Chalmers, D. K., and Thompson, P. E. (2015) Propargyloxyproline regio- and stereoisomers for click-conjugation of peptide: synthesis and application in linear and cyclic peptides. *Aust. J. Chem. 68*, 1365.

(26) Zwanziger, D., Böhme, I., Lindner, D., and Beck-Sickinger, A. G. (2009) First selective agonist of the neuropeptide Y_1-receptor with reduced size. *J. Pept. Sci. 15*, 856-866.

(27) Nguyen, T., and Francis, M. B. (2003) Practical synthetic route to functionalized rhodamine dyes. *Org. Lett. 5*, 3245-3248.

(28) Kilpatrick, L. E., Briddon, S. J., Hill, S. J., and Holliday, N. D. (2010) Quantitative analysis of neuropeptide Y receptor association with β-arrestin2 measured by bimolecular fluorescence complementation. *Br. J. Pharmacol. 160*, 892-906.

(29) Mountford, S. J., Liu, M., Zhang, L., Groenen, M., Herzog, H., Holliday, N. D., and Thompson, P. E. (2014) Synthetic routes to the Neuropeptide Y Y_1 receptor antagonist 1229U91 and related analogues for SAR studies and cell-based imaging. *Org. Biomol. Chem. 12*, 3271-3281.

(30) Holliday, N. D., Michel, M. C., and Cox, H. M. (2004) NPY receptor subtypes and their signal transduction, in *Neuropeptide Y and Related Peptides* (Michel, M. C., Ed.) pp 45-73, Springer, Berlin.

(31) Liu, M. J., Mountford, S. J., Zhang, L., Lee, I. C., Herzog, H., and Thompson, P. E. (2013) Synthesis of BVD15 peptide analogues as models for radioligands in tumour imaging. *Int. J. Pept. Res. Ther. 19*, 33-41.

(32) Michel, M. C., Beck-Sickinger, A., Cox, H., Doods, H. N., Herzog, H., Larhammar, D., Quirion, R., Schwartz, T., and Westfall, T. (1998) XVI. International Union of Pharmacology recommendations for the nomenclature of neuropeptide Y, peptide YY, and pancreatic polypeptide receptors. *Pharmacol. Rev. 50*, 143-50.

(33) Stott, L. A., Hall, D. A., and Holliday, N. D. (2016) Unravelling intrinsic efficacy and ligand bias at G protein coupled receptors: A practical guide to assessing functional data. *Biochem. Pharmacol. 101*, 1-12.

(34) Parker, E. M., Babij, C. K., Balasubramaniam, A., Burrier, R. E., Guzzi, M., Hamud, F., Gitali, M., Rudinski, M. S., Tao, Z., Tice, M., Xia, L., Mullins, D. E., and Salisbury, B. G. (1998) GR231118 (1229U91) and other analogues of the C-terminus of neuropeptide Y are potent neuropeptide Y Y_1 receptor antagonists and neuropeptide Y Y_4 receptor agonists. *Eur. J. Pharmacol. 349*, 97-105.

(35) Balasubramaniam, A., Dhawan, V. C., Mullins, D. E., Chance, W. T., Sheriff, S., Guzzi, M., Prabhakaran, M., and Parker, E. M. (2001) Highly selective and potent neuropeptide Y (NPY) Y_1 receptor antagonists based on [Pro(30), Tyr(32), Leu(34)]NPY(28-36)-NH_2 (BW1911U90). *J. Med. Chem. 44*, 1479-1482.

(36) Liu, M., Mountford, S. J., Richardson, R. R., Groenen, M., Holliday, N. D., and Thompson, P. E. (2016) Optically Pure, Structural, and Fluorescent Analogues of a Dimeric Y4 Receptor Agonist Derived by an Olefin Metathesis Approach. *J. Med. Chem. 59*, 6059-6069.

(37) Kuhn, K. K., Ertl, T., Dukorn, S., Keller, M., Bernhardt, G., Reiser, O., and Buschauer, A. (2016) High Affinity Agonists of the Neuropeptide Y (NPY) Y4 Receptor Derived from the C-Terminal Pentapeptide of Human Pancreatic Polypeptide (hPP): Synthesis, Stereochemical Discrimination, and Radiolabeling. *J. Med. Chem. 59*, 6045-6058.

(38) Kilpatrick, L. E., Briddon, S. J., and Holliday, N. D. (2012) Fluorescence correlation spectroscopy, combined with bimolecular fluorescence complementation, reveals the effects of β-arrestin complexes and endocytic targeting on the membrane mobility of neuropeptide Y receptors. *Biochim. Biophys. Acta. 1823*, 1068-1081.

Table of Contents Graphic

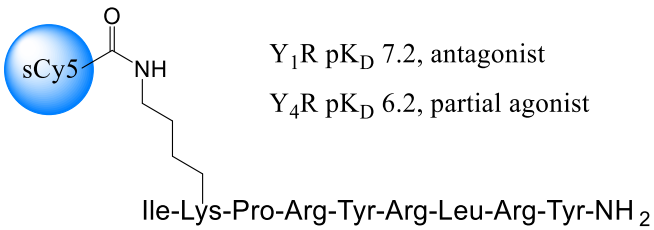

Y_1R pK_D 7.2, antagonist

Y_4R pK_D 6.2, partial agonist

[Lys^2(sCy5),Arg^4]BVD-15, **H**